Hindawi
Geofluids
Volume 2022, Article ID 6921150, 14 pages
https://doi.org/10.1155/2022/6921150

Research Article

Study on Expansion Characteristics and Expansion Potential of Gypsum Rock

Junfu Fu,[1] **Huayun Li**,[1] **Kaicheng Zhu**,[1] **Yelei Chen**,[2] **and Zhongcheng Lei**[3]

[1]*School of Architecture and Civil Engineering, Xihua University, Chengdu 610039, China*
[2]*School of Civil Engineering, Southwest Jiaotong University, Chengdu 610031, China*
[3]*Shenzhen Municipal Design and Research Institute Co., LTD., Shenzhen 518029, China*

Correspondence should be addressed to Kaicheng Zhu; zhukaicheng@stu.xhu.edu.cn

Received 9 September 2022; Revised 23 September 2022; Accepted 27 September 2022; Published 14 October 2022

Academic Editor: Dongjiang Pan

In this study, the relationship between four expansion indices and the expansion potential of gypsum rock was studied; on this basis, a criterion for judging expansion potential is established for gypsum rock. The results show that the free expansion rate is unsuitable for grading gypsum rocks' expansion potential. Setting the gypsum rock in the Wuzhishan tunnel as the research subject, the ultimate expansion rate is 24.28% on the 7th day and 34.08% on the 30th day; the ultimate expansion rate on the 7th day of the indoor rock sample can be estimated by the fitting formula on the 30th day, the ultimate expansion force is 304.51 kPa, and the BET-specific surface area is 6.31 m^2/g. The ultimate expansion ratio and BET-specific surface area have an excellent linear relationship with the ultimate expansion force. Setting the ultimate expansion force, ultimate expansion ratio and BET-specific surface area as the standard, the criterion for judging the expansion potential of gypsum rock is determined, which is more convenient and accurate than existing standards. The standard in this paper can predict the potential disasters that may occur in underground engineering.

1. Introduction

Different rock layers have different effects on engineering structures [1–3], and some indicators can be used to predict the possible effects [4], such as landslide prediction and tunnel lining failure prediction [5–8]. In the construction of expansive rock strata, after contact with water, the expansive compressive effect of expansive rock will influence the safety of the engineering structure, and the expansion potential is one of the important indicators for designers to judge the expansive compressive effect, making it crucial to the normal construction and safe operation of engineering structures [9–12].

At present, expansive rocks are divided into two categories [13–18]: the first one is caused by chemical expansion reaction, the mechanism is complex, and the time is long (such as anhydrite and glauberite); the second one is caused by hydrophilic minerals, and the expansion of this type of rock is cyclically reciprocated under the action of water absorption and loss (such as mudstone and tuff) [19]. The main indicators for judging the expansion potential of expansive rocks include water content [20–22], viscous material content [9, 15, 23–25], free expansion rate [25], ultimate expansion rate [26], dry saturated water absorption rate [27], and ultimate expansion force [9, 25].

Most of the criteria for the above indicators are determined based on the test results of the second type of expansive rock, which are not suitable for the first type of rock. Gypsum rock is the first type of expansive rock, and it contains anhydrite ($CaSO_4$), plaster of paris ($CaSO_4$•H_2 O), and hemihydrate gypsum ($CaSO_4$•$0.5H_2O$); these three minerals will be converted into Gypsum ($CaSO_4$•$2H_2O$). The increase of crystal water leads to the expansion of crystal structure and then increases the volume of rock samples [28–34].

Abu [30] studied the expansion characteristics of gypsum rocks and clay minerals in Egypt and found that the water absorption of montmorillonite mainly causes the expansion of clay minerals, and the key factor for the expansion of gypsum rocks is the anhydrite. The expansiveness of rock is proportional to the anhydrite content. Ma et al. [29]

Table 1: Sample processing.

Serial number	Process mode
A	Put sample A into distilled water to fully absorb water; then remove excess water and leave the sample indoor to dry, and grind the sample to powder with a disintegrator and pass through a 0.5 mm sieve; finally, place the powder in an oven to dry at 75°C for 48 hours and store
B	Add 400 g of distilled water to sample B, and then seal the chamber until the water absorption is completed. After grinding to powder with a disintegrator and passing through a 0.5 mm sieve, it was then placed in an oven to dry at 75°C for 48 hours
C	Add 200 g of distilled water to sample C, and then seal the chamber until the water absorption is completed. After grinding to powder with a disintegrator and passing through a 0.5 mm sieve, it was then placed in an oven to dry at 75°C for 48 hours and store
D	Keep sealing the sample
E	Place sample D in an oven to dry at 220°C for 48 hours and store

analyzed the effect of $CaSO_4 \cdot H_2O$ composition on four different gypsum rocks; it was found that the higher the content of $CaSO_4 \cdot H_2O$ composition, the lower the strength and energy change of gypsum rocks, but the larger the microscopic size of rock samples. Xu et al. [16] studied the expansion characteristics of rerigid gypsum rock and found that its maximum expansion rate in a short time was 2.6%. Wu [18] conducted a short-term laboratory test to analyze the expansion characteristics of the remolded gypsum rock. The free expansion rate was 3.5%, the expansion rate was 6.01%, and the expansion force was 2.20 kPa. However, the predicted ultimate expansion force can reach up to 824 kPa based on its linear expansion coefficient. Azam et al. [28] analyzed the porosity and $CaSO_4$ content of gypsum rock by XRD and SEM to evaluate the expansion characteristics of gypsum rock microscopically, and it was concluded that its expansion force could reach up to 1660 kPa. Rauh et al. [35] used a remolded sample of anhydrite to analyze the expansion characteristics and found that the expansion of the rock mainly depends on the crystallinity.

According to literatures [10, 18, 28, 36], the expansion stress of gypsum rock can be increased by more than ten times after a few years, so the short-term expansion rate and expansion force are not accurate in evaluating its expansion potential. If the expansion potential is incorrectly estimated, the initially designed strength of the project structure will not be enough, which may lead to a potential safety hazard for the safe operation of the project later [36]. Chang et al. [37] used software to analyze the causes of landslides. Huang et al. [38] use environmental factors to guide machine self-learning to predict landslides. Therefore, in this paper, the free expansion rate test, the ultimate expansion rate test, the ultimate expansion force test, and the BET-specific surface area test were carried out on the gypsum rock from the Wuzhishan Tunnel; at the same time, based on the existing methods [13, 14, 18, 30], the expansion potential of gypsum rocks can be quickly and accurately predict by combining the ultimate expansion rate and specific surface area indexes.

2. Materials and Methods

2.1. Rock Sample Pretreatment. The rock samples were obtained from the gypsum surrounding rock section of Wuzhishan Tunnel. In order to obtain gypsum rocks with different expansion potentials, remolded samples are used in the tests of expansion characteristic index [15–18, 39, 40]. Although the sample used in this paper is the remolded sample, the expansion of gypsum rock is due to the volume expansion caused by the increase of crystal water. The cellular structure of gypsum rock is not damaged in the process of remolding, so the expansion potential of the rock sample is not affected. Besides, the expansion time of gypsum rock is extremely long, and the remolded sample can be used to shorten the expansion time so as to get the ultimate expansion force and ultimate expansion rate. Therefore, it is meaningful to use remolded gypsum rock samples for research in this paper.

The gypsum rock collected on site was ground into powder, passed through a 0.5 mm sieve, and then was divided into 5 groups (every group weights 2 kg), which were numbered A, B, C, D, and E, respectively. Five groups of samples were pretreated, as shown in Table 1.

Finally, each group was evenly divided into two parts.

2.2. X-Ray Photoelectron Spectroscopy and X-Ray Fluorescence Spectroscopy. In the X-ray Photoelectron Spectroscopy (XPS) test, ESCALAB Xi+ XPS developed by Thermoscientific Company (as shown in Figure 1) was used for qualitative and quantitative analysis of gypsum rock [41–43]. The X-ray gun uses an Al target with relatively high intensity. The data obtained from the test was firstly analyzed by the software and then compared with the existing element database. The X-Ray Fluorescence (XRF) analysis was performed using the Zetium (XRF) instrument from PANalytical, the Netherlands, as shown in Figure 2. Refer to the literature for XRF test process [44–47].

2.3. Expansion Characteristics Test

2.3.1. Free Expansion Rate. The free expansion rate is defined as the percentage of the volume change after the expansion to the initial volume when weathered expansive rock particles with a certain amount are placed in water without any constraints [48]. The free expansion rate is related to the content of hydrophilic minerals and the thickness of particles, which can reflect the expansion performance of expansive rocks to a certain extent. Therefore, it

Figure 1: XPS test system.

Figure 2: XRF test system.

is often used as one of the indicators to judge the expansion potential. The free expansion rate test was carried out according to the specification [49, 50]. The test process and data processing refer to the standard [51]. Free expansion rate test steps are as follows:

Figure 3: The dilatometer.

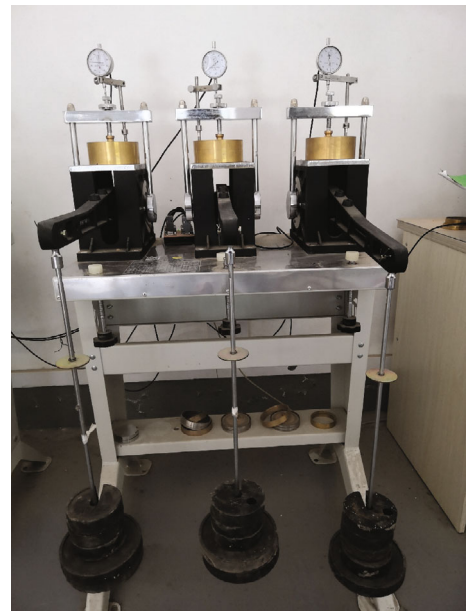

Figure 4: Expansion force testing instrument.

(Step 1) Clean the measuring cylinder, agitator, and measuring cup; then dry and set aside.

(Step 2) The vector earth cup is loaded with sufficient gypsum rock powder.

(Step 3) Put the following components into the 50 mL measuring cylinder in turn: 30 mL distilled water and 5 mL 5% NaCl solution, and the sample in the measuring cup. Then, stir 10 times along the vertical direction of the cylinder.

(Step 4) The stirrer is rinsed with distilled water in the cylinder and then infused with distilled water to 50 mL along the cylinder wall.

(Step 5) Stay for a while, and then, the readings are recorded.

Figure 5: JW-BK132F instruments.

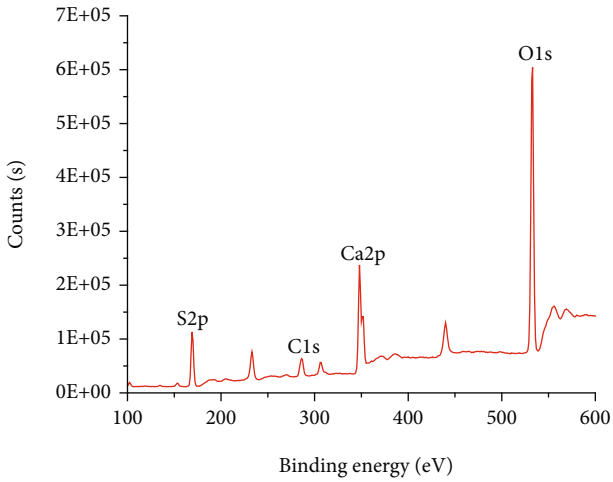

Figure 6: XPS map of gypsum rocks.

Table 2: Percentage of oxide content in gypsum rock.

Oxide	Content percentage	Oxide	Content percentage	Oxide	Content percentage
SO_3	56.438%	MgO	1.219%	Fe_2O_3	0.058%
CaO	39.703%	SrO	0.395%	Na_2O	0.047%
SiO_2	1.964%	Al_2O_3	0.143%	K_2O	0.023%

2.3.2. Ultimate Expansion Rate. Under lateral confinement, the remolded sample had an expansion reaction through the slow contact between the permeable stone and the water from top to bottom [50, 52, 53]. The ratio of the axial increased amount after expansion to the initial amount is defined as the ultimate expansion ratio. The limit expansion rate and the free expansion rate are both judging indicators of the expansion potential, and their difference is that in the limit expansion rate test, the sample is chemically reacted with the water in the permeable stone, and the contact area between the sample and the water is larger, slowing the expansion and the surface hardening, which will affect the expansion of the internal gypsum rock powder. The expansion ratio test apparatus is shown in Figure 3. The test process and data processing refer to the standard [51, 54]. The expansion rate test steps are as follows:

(Step 1) The ring cutter and pervious stone were cleaned and dried; then, the pervious stone was buried in gypsum rock powder for 60 minutes.

(Step 2) After adding gypsum rock powder of 1/3 of its height into the ring cutter each time, compaction is carried out until the sample height is flush with the ring cutter.

(Step 3) Assemble expander, adjust dial gauge, and record initial reading.

(Step 4) Add distilled water to the water box, and the water level is 5 mm higher than the sample. Record the dial gauge reading after a period of time. Disassemble the dilatometer, and sort out the test instruments.

2.3.3. Ultimate Expansion Force. Under the limitation of the surrounding rock and soil, the increase of the water absorption volume of expansive rock or expansive soil will produce a limiting reaction force, which is called the expansion force [48, 50, 55–57]. In this test, the expansion force measured by the gypsum rock remolded sample is under the limit condition. The test adopts a WG single-lever consolidation instrument, as shown in Figure 4. The test process and data processing refer to the standard [51]. The steps of expansion force test are as follows:

(Step 1) The ring cutter and pervious stone were cleaned and dried; then, the pervious stone was buried in gypsum rock powder for 60 minutes.

Figure 7: Before expansion.

Figure 8: After Expansion.

(Step 2) After adding gypsum rock powder of 1/3 of its height into the ring cutter each time, compaction is carried out until the sample height is flush with the ring cutter.

(Step 3) Add distilled water to the water box, and the water level is 5 mm higher than the sample.

(Step 4) When the sample begins to expand and the expansion is not higher than 0.01 mm, add the load to make the gauge recover the initial reading. Excessive disturbance to the sample should be avoided when adding the charge.

(Step 5) With the 24-hour deformation as the boundary, the charge returns the scale to the previous 24-hour deformation position. After a period of time, the test was terminated and the load value was recorded.

2.4. BET-Specific Surface Area. Specific surface area (A_s) refers to the total surface area of solid particles per unit mass, and it is one of the important indicators for analyzing the coupling effect of liquid-solid and liquid-gas interfaces. In recent years, with the further study of expansive rock and soil from macro to micro, the specific surface area has been more focused [49, 58–66], which can reflect the expansion characteristics and expansion potential of expansive rock and soil. At present, there are many studies on the specific surface area of expansive soil [49, 58, 59, 63, 67, 68], while there are few studies on expansive rocks [60], especially the specific surface area of the first type of expansive rocks.

This paper studies the specific surface area of gypsum rock based on the indoor nitrogen adsorption test. In the nitrogen adsorption method [69], when nitrogen is liquid at low temperature, it can be adsorbed on the surface of powder particles. After room temperature is recovered, the liquid nitrogen returns to a gaseous state and is detached from the surface of the powder particles. By measuring the gaseous nitrogen, the specific surface area of the powder particles completely wrapped by a layer of liquid nitrogen can be obtained.

In fact, nitrogen is adsorbed on the surface of powder particles in multiple layers. According to the saturated adsorption amount of nitrogen in a single layer, combined with thermodynamics and kinetics, the actual adsorption amount of nitrogen can be accurately obtained, that is, the multilayer adsorption theory (BET) equation, as shown in Equation (1). The BET equation is a calculation method of nitrogen adsorption method, which can accurately calculate the actual adsorption amount of nitrogen, so it is widely used in the determination of specific surface area.

$$P/V(P_0 - P) = 1/V_m \bullet C + (C-1)P/V_m \bullet C \bullet P_0 \quad (1)$$

where V is the actual adsorption amount of nitrogen, P_0 is the saturated vapour pressure, P is the partial pressure of nitrogen, V_m is the monolayer saturated adsorption amount of nitrogen, and C is a material constant.

The five groups of samples A, B, C, D, and E were ground with a natural agate grinder, then passed through a 500-mesh sieve, and 2 g of each group of samples were collected and sealed. In the specific surface area test, the JW-BK132F-specific surface area and pore size analyzer

Table 3: Test results of free expansion rate.

Sample number	Time (h)	Initial volume (mL)	Expanded volume (mL)	Free expansion rate (%)	
				Experimental value	Average value
A-1	722.0	9.9	10.0	1.01	1.51
A-2	722.0	10.0	10.2	2.00	
B-1	721.0	10.1	10.3	1.98	2.45
B-2	721.0	10.3	10.6	2.91	
C-1	715.0	9.7	10.2	5.15	5.13
C-2	715.0	9.8	10.3	5.10	
D-1	723.0	9.9	10.6	7.07	7.11
D-2	723.0	9.8	10.5	7.14	
E-1	721.0	9.9	10.9	10.10	10.55
E-2	721.0	10.0	11.0	11.00	

produced by Jingwei Gaobo Company are used, as shown in Figure 5.

3. Results

3.1. Mineral Composition. The XPS spectrum of gypsum rock can be obtained, as shown in Figure 6. It can be seen from Figure 6, each element's peak area and sensitivity factor were quantitatively analyzed, and the percentage of gypsum rock element content was obtained after normalization. The highest atomic percentage of O element is 61.61%, and the lowest atomic percentage of Ca element is 12.20%. Therefore, the content of $CaSO_4$ was higher than that of $CaSO_4{\cdot}_2H_2O$. In order to analyze the content of $CaSO_4$ and $CaSO_4{\cdot}2H_2$ O accurately, the samples were then subjected to XRF.

The percentage of oxide content of gypsum rock is shown in Table 2. According to the existing data [18, 29, 30, 35, 39], the theoretical percentages of CaO and SO_3 in gypsum ($CaSO_4{\cdot}2H_2O$) are 32.6% and 46.5%, respectively, while their percentages in anhydrite ($CaSO_4$) are 41.2% and 58.8%, respectively.

As shown in Table 2, the percentage of CaO in the gypsum rock of the Wuzhishan Tunnel is 39.703%, and the percentage of SO_3 is 56.438%; their contents are between the theoretical percentages of gypsum and anhydrite, but close to the theoretical percentages of anhydrite, which further verifies the conclusion obtained by XPS analysis, so the rock sample is not a single gypsum rock or anhydrite but a gypsum rock composed of a mixture of the two, and the content of anhydrite ($CaSO_4$) is more than that of gypsum ($CaSO_4{\cdot}2H_2O$).

3.2. Expansion Characteristic Index

3.2.1. Free Expansion Rate. The gypsum rock powder before and after free expansion is shown in Figures 7 and 8. The free expansion rate test results are shown in Table 3. It can be seen from Table 3 that the free expansion rate of the samples in group A is the lowest, with an average value of 1.51%; the free expansion rate of the samples in group E is the highest, with an average value of 10.55%. With the deepening of the hydration degree, the free expansion rate of gypsum rock also decreases, and the shrinkage reaches a maximum of 9.04%.

In this test, the highest free expansion rate is 10.55%; it is found that gypsum rock does not belong to the expansive rock compared with most expansion classification standards, which is obviously contrary to the existing research [16, 17, 28, 39]. At the same time, in the free expansion rate test, it was found that the gypsum rock powder occurred to harden, as shown in Figure 9; the upper anhydrite in the graduated cylinder hydrated into gypsum and hardened, resulting in a weakened reaction between the lower anhydrite and water, which in turn decreased the free expansion rate of gypsum rock. Therefore, it is not accurate to judge the expansion potential of gypsum rock by the free expansion rate.

3.2.2. Ultimate Expansion Rate. The test results of the ultimate expansion rate are shown in Table 4. The gypsum rock sample before and the confining expansion is shown in Figures 10 and 11.According to the comparison of the top and side views of the sample before and after the expansion, it is found that the upper and lower parts of the ring knife have a prominent expansion of the sample, and the upper part has the most significant expansion and the surface is rich in water, suggesting that the ultimate expansion rate test does not appear phenomenon similar to the free expansion rate test.

According to the ultimate expansion ratio in Table 4, it can be seen that on the 7th and 30th days, the expansion ratio of the samples of group A is the smallest, with an average value of 1.83% and 3.05%, respectively; on the 7th and 30th days, the expansion ratio of the samples of group E is the largest, with an average value of 27.95% and 42.13%. The maximum expansion rate and the minimum expansion rate differ by about 14 times; with the deepening of the hydration degree, the expansion rate of the sample decreases. Compared with the free expansion rate, the results of the ultimate expansion rate test are more valuable.

During the test of the ultimate expansion rate of gypsum rock, the change of the expansion rate showed a trend of first increasing and then decreasing, with an obvious inflexion point. According to the statistics of 10 groups of data, the

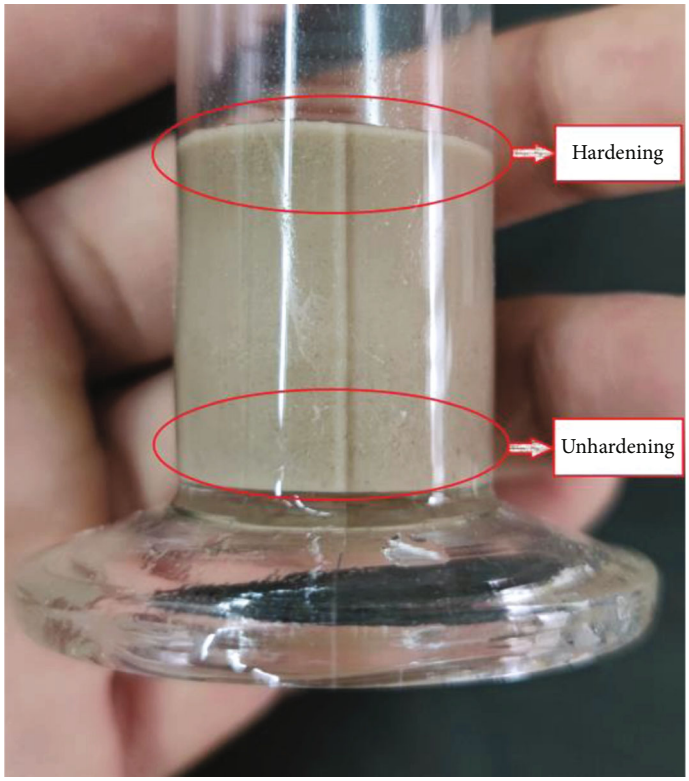

Figure 9: The hardening of Gypsum rock powder.

Table 4: Test results of ultimate expansion rate.

Sample number	The reading of the dial gauge (mm)			Expansion rate (%)		Average expansion rate (%)	
	0 days	7 days	30 days	7 days	30 days	7 days	30 days
A-1	9.00	9.41	9.65	2.05	3.25	1.83	3.05
A-2	9.00	9.32	9.57	1.60	2.85		
B-1	4.00	5.53	6.03	7.65	10.15	6.93	9.68
B-2	4.00	5.24	5.84	6.20	9.20		
C-1	5.00	8.26	9.85	16.30	24.25	15.35	24.08
C-2	5.00	7.88	9.78	14.40	23.90		
D-1	5.00	9.36	11.50	21.80	32.50	24.28	34.08
D-2	5.00	10.35	12.13	26.75	35.65		
E-1	5.00	10.53	13.73	27.65	43.65	27.95	42.13
E-2	5.00	10.65	13.12	28.25	40.60		

inflexion point was basically shown in the range from the 5th day to the 7th day. Therefore, considering the worst case, the 7th day is considered the moment when the inflexion point appears, and its expansion rate is recorded. By analyzing the ultimate expansion rate of the sample on the 7th day and the 30th day, a certain linear relationship is found. The fitting curve is shown in Figure 12, and the linear relationship is shown in

$$\delta_{30t} = 1.45\delta_{7t} + 0.41\ R^2 = 0.964, \tag{2}$$

where δ_{30t} is the expansion rate on the 30th day (%) and δ_{7t} is the expansion rate on the 7th day (%).

In the limit expansion rate test, there is a good fitting relationship between the expansion rate on the 7th day and the expansion rate on the 30th day, and the expansion rate on the 30th day can be predicted by the expansion rate on the 7th day, which greatly saves the test time.

3.2.3. Ultimate Expansion Force. The test results of the ultimate expansion force of gypsum rock are shown in

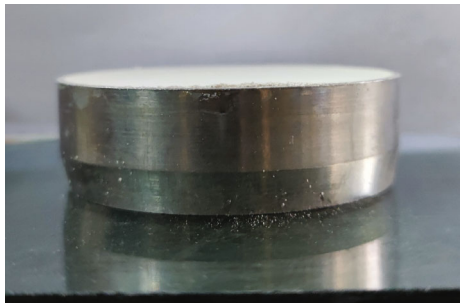

Figure 10: Before the confined expansion.

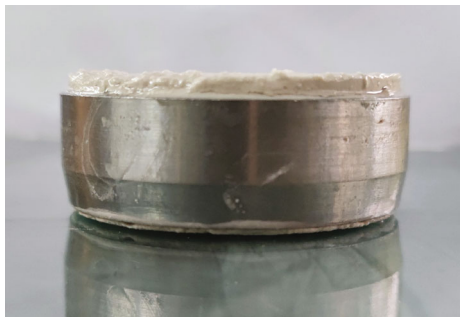

Figure 11: After the confined expansion.

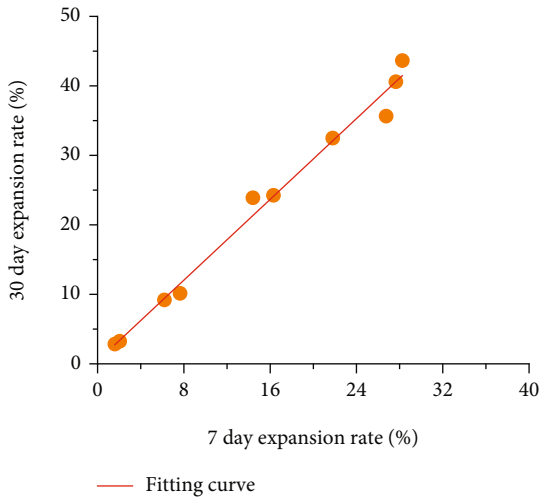

Figure 12: Fitting curve of expansion rate on the 7th day and the 30th day.

Table 5; it can be seen that the expansive force of gypsum rock is up to 387.57 kPa, and the lowest is only 15.81 kPa; the difference between the expansive force of group A and group E is about 23 times. Anhydrite content leads to a big difference in swelling force between the two groups. Group A contains less anhydrite after treatment, while group E contains mostly anhydrite after treatment. The ultimate expansion force is negatively correlated with the degree of hydration of the sample.

Table 5: Ultimate expansion force test results.

Sample number	Time (d)	Expansion force (kPa)	
		Experimental value	Average value
A-1	30	16.73	16.27
A-2	30	15.81	
B-1	30	83.24	82.20
B-2	30	81.15	
C-1	30	147.36	145.98
C-2	30	144.59	
D-1	30	296.54	304.51
D-2	30	312.47	
E-1	30	387.57	374.93
E-2	30	362.28	

3.3. BET-Specific Surface Area. The five groups of gypsum rock samples were tested twice for the BET-specific surface area, and five pairs of P/P_0 and $P/V(P_0 - P)$ data were collected each time. The BET-specific surface area curve can be drawn through these 5 pairs of data, as shown in Figure 13.

It can be seen from Figure 13 that the $P/V(P_0 - P)$ of the sample A-2 is the largest, which is 1.01; the $P/V(P_0 - P)$ of the sample D-2 is the smallest, which is 0.30. The P/P_0 of each point in groups A, B, C, D, and E is in the range of 0.05~0.35 and has a good linear relationship with the $P/V(P_0 - P)$, which is in line with the requirements for multipoint determination of BET-specific surface area in the specification [70]. According to the linear relationship between the $P/V(P_0 - P)$ and P/P_0 of each group in Figure 13, combined with the specification, the specific surface area of gypsum rock can be obtained, as shown in Table 6.

It can be seen from Table 6 that the BET-specific surface area of sample A-2 is the smallest, which is 1.68 m^2/g; the specific surface area of sample E-1 is the largest, which is 8.21 m^2/g. According to the change of BET-specific surface area from group A to group E, it can be found that the BET-specific surface area is negatively correlated with the hydration degree; this is because the anhydrite ($CaSO_4$) in gypsum rock converts into gypsum ($CaSO_4 \cdot H_2O$) after absorbing water, which manifests as an increase in unit cells in microscopic aspect and an increase in the volume of rock powder particles in macroscopic aspect.

By analyzing the BET-specific surface area of the gypsum rock, it is concluded that the content of anhydrite affects the BET-specific surface area, indicating that the specific surface area of the gypsum rock is related to its expansion characteristics. Therefore, the expansion potential of gypsum rock samples can also be reflected by the BET-specific surface area.

4. Discussion

4.1. Expansive Rock Classification. Expansion potential refers to the expansion capacity of expansive rock and soil after

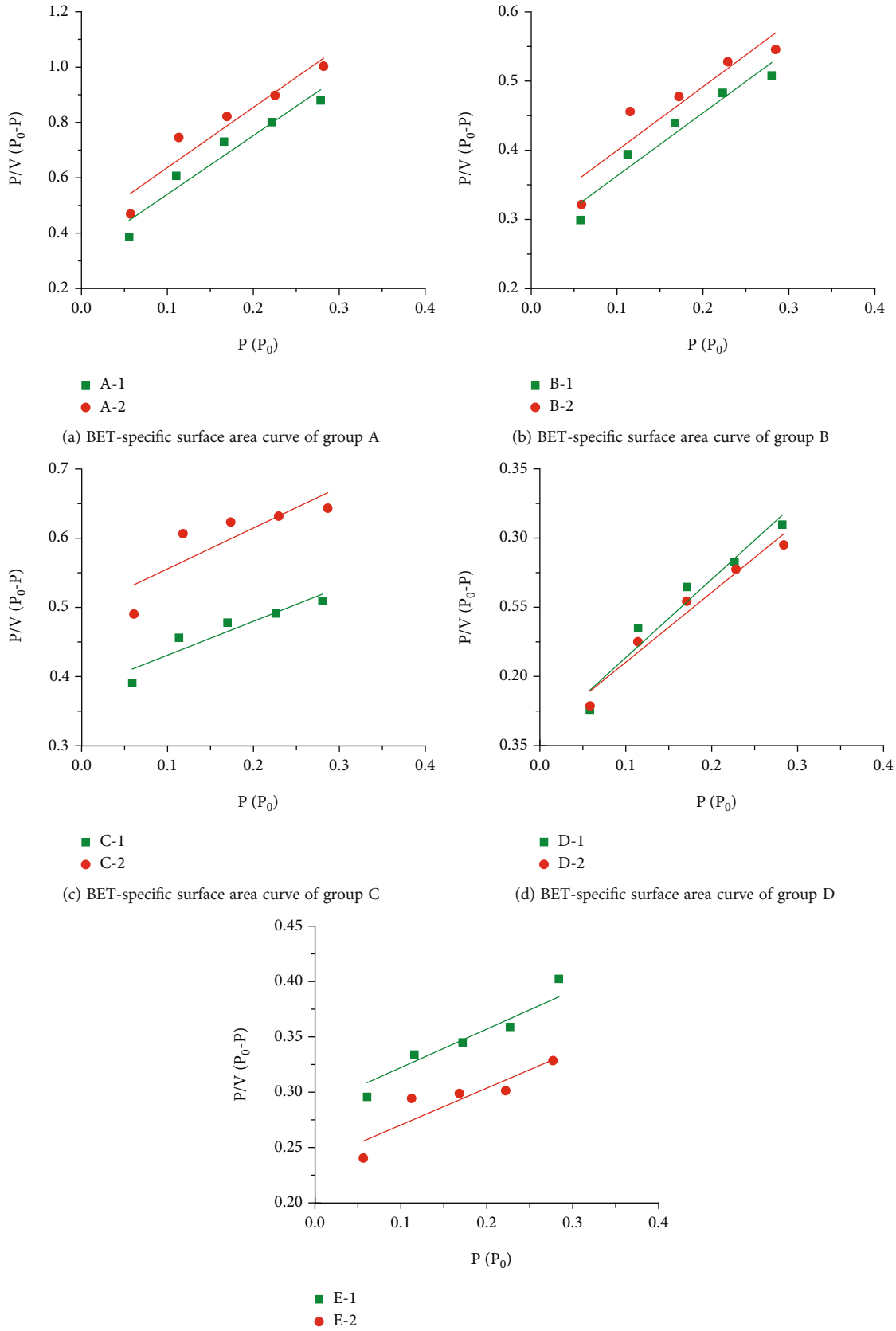

(a) BET-specific surface area curve of group A

(b) BET-specific surface area curve of group B

(c) BET-specific surface area curve of group C

(d) BET-specific surface area curve of group D

(e) BET-specific surface area curve of group E

Figure 13: BET-specific surface area curve of gypsum rock samples.

Table 6: BET-specific surface area test results of gypsum rock.

Sample number	α (inclination)	β (intercept)	Specific surface area (m^2/g)	
			Experimental value	Average value
A-1	2.12	0.33	1.78	1.73
A-2	2.17	0.42	1.68	
B-1	0.91	0.27	3.69	3.62
B-2	0.92	0.31	3.55	
C-1	0.49	0.38	4.99	4.60
C-2	0.52	0.52	4.20	
D-1	0.57	0.16	6.04	6.31
D-2	0.51	0.16	6.57	
E-1	0.24	0.29	8.21	7.93
E-2	0.33	0.24	7.65	

absorbing water. The determination of expansion potential is essential in engineering design, and an inaccurate evaluation will affect the structural safety of engineering. Therefore, it is necessary to use suitable methods and indicators to judge the expansion potential of different types of expansive rock and soil.

4.2. Expansion Potential Determination of Gypsum Rock

4.2.1. Selection of Judgment Indicators. According to the test results of the free expansion rate, combined with Table 7, it is judged that the gypsum rock is not an expansive rock. This is because, in the test, the hydration of the upper anhydrite results in a weakened reaction between the lower anhydrite and water, which in turn causes a low free expansion rate of gypsum rock. Therefore, although the free expansion [25] rate is one of the most widely used judging indicators for expansive rock and soil, it is not suitable for judging the expansion potential of gypsum rock.

In the ultimate expansion rate test [26], the samples did not show the phenomenon of surface hardening agglomeration hindering the water absorption of the internal sample, and the ultimate expansion rate was as high as 43.65%, indicating that the ultimate expansion rate can be used as a grading index of the expansion potential of gypsum rocks. However, the classification standard in Table 6 is mainly based on the expansion mechanism of the second type of expansive rock, while gypsum rock belongs to the first type of expansive rock, and their expansion mechanism is completely different; therefore, it needs to be corrected when the limit expansion coefficient is used as the judgment index of the expansion potential of gypsum rock.

The ultimate expansion force [13, 14, 39] is not only the most important index for judging the expansion potential of expansive soil but also the most important parameter for structural design. No matter the reason for the expansion, its ultimate expansion force corresponds to the same expansion potential grade; the mineral composition and expansion mechanism only affect the expansion rate and do not affect the expansion potential grade. Therefore, the expansion potential grade of gypsum rock concerning the ultimate expansion force can be judged regarding Table 7.

For the first type of expansive rock and the second type of expansive rock, the meaning of the specific surface area is different. For the first type of expansive rock, the change in the specific surface area is due to the hydration of anhydrite, and the number of unit cells increases from 4 to 8, resulting in a larger specific surface area of the rock sample before expansion [18]. For the second type of expansive rock, the specific surface area affects the range of the contact surface between hydrophilic minerals and water. In the test of the specific surface area of gypsum rock, it is found that the specific surface area is related to the expansion potential of gypsum rock, but the current expansion potential judgment based on specific surface area is based on the range determined by the second type of expansive rock, which is not suitable for gypsum rock. Therefore, when the BET-specific surface area is used as the evaluation index of the expansion potential of gypsum rock, it is necessary to redivide its grade range.

In this paper, the ultimate expansion ratio, ultimate expansion force, and specific surface area are selected to divide the expansion potential of gypsum rock based on laboratory tests.

4.2.2. The Relationship between the Ultimate Expansion Rate and the Ultimate Expansion Force. The relationship curve between the ultimate expansion rate of gypsum rock (Table 4) and the test results of the ultimate expansion force (Table 5) can be drawn from the test results, as shown in Figure 14. It can be seen from Figure 14 that the ultimate expansion rate of gypsum rock is positively correlated with the ultimate expansion force, and there is a certain functional relationship as follows:

$$P_s = 9.05\delta_{30t} - 19.83\ R^2 = 0.961, \tag{3}$$

where P_s is the ultimate expansion force (kPa) and δ_{30t} is the 30th day ultimate expansion rate (%).

From Equation (3), it can be seen that the fitting degree between the ultimate expansion ratio and the ultimate expansion force is relatively high, and the ultimate expansion force of the specimen can be estimated from the ultimate unloaded expansion ratio of the sample through this formula.

4.2.3. Relationship between Specific Surface Area and Ultimate Expansion Force. The BET-specific surface area test results of gypsum rock (Table 6) and the ultimate expansion force test results (Table 5) are analyzed, and their relationship curve is obtained, as shown in Figure 15. Figure 15 shows that the expansion force increases synchronically with the BET-specific surface area increase, showing a good linear relationship, and the fitting formula of the primary function can be obtained:

$$P_s = 61.48A_s - 112.54\ R^2 = 0.963, \tag{4}$$

Table 7: Main classification standards of expansive rock [13, 14, 18, 39].

Indicator	Nonexpansive rock	Slight expansive rock	Weak expansive rock	Strong expansive rock
Free expansive rate (%)	<30	30~50	50~70	>70
Dry saturated water absorption (%)	<10	10~30	30~50	>50
Linear shrinkage (%)	<5	5~8	8~12.5	>12.5
Ultimate expansive rate (%)	<5	5~10	10~20	>20
Ultimate expansive force (kPa)	<100	100~300	300~500	>500
Specific surface area (m^2/g)	<50	50~100	100~300	>300
Exchanging volume (mL/g)	<0.1	0.1~0.2	0.2~0.5	>0.5
Strength of surrounding rock (MPa)	>1	0.7~1	0.4~0.7	<0.4

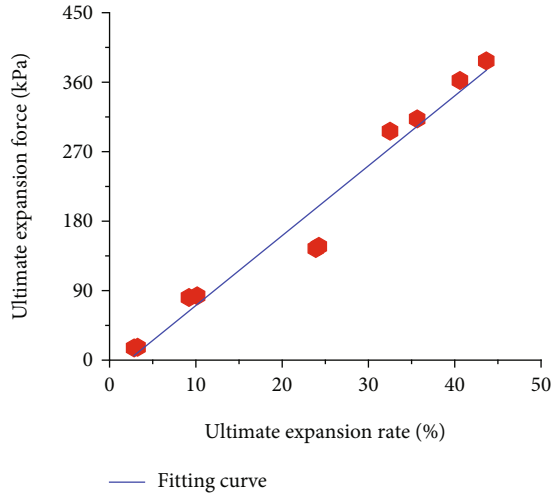

Figure 14: Relation curve between ultimate expansion rate and ultimate expansion force.

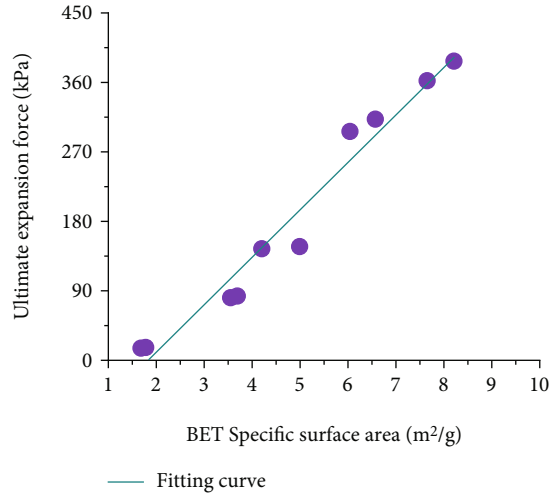

Figure 15: The relationship between BET-specific surface area and expansion force.

where P_s is the ultimate expansion force (kPa) and A_s is the BET-specific surface area (m^2/g).

4.2.4. Expansion Potential Classification. According to the ultimate expansion force in Table 7, the classification range of the expansion potential is divided into non, slight, weak, and strong, and the corresponding ultimate expansion force ranges are <100 kPa, 100~300 kPa, 300~500 kPa, and >500 kPa. According to Formula (3), the limit expansion rate ranges are obtained as <13.3%, 13.3~35.3%, 35.3~57.4%, and >57.4%. According to Formula (4), the range of BET-specific surface area is <3.5m^2/g, 3.5~6.7 m^2/g, 6.7~10.0 m^2/g, and

Table 8: Classification of the expansion potential of gypsum rocks.

Judgement indicators	Nonexpansive rock	Weak expansive rock	Intermediate expansive rock	Strong expansive rock
Ultimate expansive rate (%)	<13.3	13.3~35.3	35.3~57.4	>57.4
Ultimate expansive force (kPa)	<100	100~300	300~500	>500
BET-specific surface area (m^2/g)	<3.5	3.5~6.7	6.7~10.0	>10.0

>10.0m^2/g. Thus, the classification standard of gypsum rock expansion potential can be obtained, as shown in Table 8.

The BET-specific surface area of the sample was tested indoors for 2 to 3 hours; at the same time, the expansion ratio test was carried out for 7 days, and then, the expansion ratio for 30 days was converted using Equation (1). Combined with Table 8, the expansion potential of gypsum rock can be quickly and accurately analyzed. Compared with the traditional method of judging the expansion potential which lasts for several months, the criterion in this paper can greatly save time and ensure the rapid and safe construction of the project. The ultimate expansion rate, ultimate expansion force, and BET-specific surface area of the gypsum rock in the Wuzhishan Tunnel are 34.08%, 304.51 kPa, and 6.31 m^2/g, respectively. According to the standards in this paper, the rock is judged to be intermediate expansive rock.

The division of expansion potential is for reference to engineering practice. In the future research, the expansion potential should be adjusted after observing the expansion force changes of the field engineering structures.

5. Conclusions

In this research, the expansion characteristics and BET-specific surface area of gypsum rock are analyzed, and the standard for judging the expansion potential of gypsum rock is established. The main conclusions are as follows:

(1) Through XPS and XRF analysis, it was confirmed that the surrounding rock of the Wuzhishan Tunnel is gypsum rock, and the content of anhydrite is much higher than that of gypsum

(2) In the test, the maximum expansion rate is 42.13%, the maximum expansion force is 374.93 kPa, and the maximum specific surface area is 7.93 m^2/g. The hydration degree of gypsum rocks is negatively correlated with free expansion rate, ultimate expansion rate, ultimate expansion force, and BET-specific surface area

(3) It is found that the free expansion rate is not suitable to judge the expansion potential of gypsum rock. The criteria for judging the expansion potential of gypsum rock by the ultimate expansion force, ultimate expansion ratio, and BET-specific surface area are established. This criterion can more accurately judge the real expansion potential of gypsum rock. According to this standard, the gypsum rock of the Wuzhishan tunnel is determined as the weak expansive rock

Data Availability

The data used to support the findings of this study are available from the corresponding author upon request.

Conflicts of Interest

No potential conflict of interest was reported by the author(s).

References

[1] Z. Chang, Z. Du, F. Zhang et al., "Landslide susceptibility prediction based on remote sensing images and GIS: comparisons of supervised and unsupervised machine learning models," *Remote Sensing*, vol. 12, no. 3, p. 502, 2020.

[2] F. Mugagga, V. Kakembo, and M. Buyinza, "A characterisation of the physical properties of soil and the implications for landslide occurrence on the slopes of mount Elgon, Eastern Uganda," *Natural Hazards*, vol. 60, no. 3, pp. 1113–1131, 2012.

[3] E.-S. S. Abu Seif and A. A. Bahabri, "Rockfall hazards assessment along the Aswan–Cairo highway, Sohag Governorate, Upper Egypt," *Natural Hazards*, vol. 99, no. 2, pp. 991–1005, 2019.

[4] F. Huang, Z. Cao, J. Guo, S.-H. Jiang, S. Li, and Z. Guo, "Comparisons of heuristic, general statistical and machine learning models for landslide susceptibility prediction and mapping," *Catena*, vol. 191, p. 104580, 2020.

[5] S.-H. Jiang, J. Huang, F. Huang, J. Yang, C. Yao, and C.-B. Zhou, "Modelling of spatial variability of soil undrained shear strength by conditional random fields for slope reliability analysis," *Applied Mathematical Modelling*, vol. 63, pp. 374–389, 2018.

[6] Z. Guo and Z. Zhao, "Numerical analysis of an expansive subgrade slope subjected to rainfall infiltration," *Bulletin of Engineering Geology and the Environment*, vol. 80, no. 7, pp. 5481–5491, 2021.

[7] C. Butscher, S. Breuer, and P. Blum, "Swelling Laws for clay-sulfate rocks revisited," *Bulletin of Engineering Geology and the Environment*, vol. 77, no. 1, pp. 399–408, 2018.

[8] X. Li, Y. Wang, Y. Hu, C. Zhou, and H. Zhang, "Numerical investigation on stratum and surface deformation in underground phosphorite mining under different mining methods," *Frontiers in Earth Science*, vol. 10, p. 831856, 2022.

[9] M. Gysel, "Design of Tunnels in swelling rock," *Rock Mech Rock Engng*, vol. 20, no. 4, pp. 219–242, 1987.

[10] G. G. Gschwandtner, U. Kahn, B. Kohlböck, B. Moritz, and S. Wagner, "Granitztal tunnel chain – experience from the construction of the Langer Berg Tunnel and challenges in the anhydrite zone," *Geomechanik und Tunnelbau*, vol. 10, no. 6, pp. 730–739, 2017.

[11] A. Zettler, R. Poisel, A. Preh, and H. Konietzky, "Tunnelling in swelling rock – a solved problem," *Geomechanik Tunnelbau*, vol. 3, pp. 557–566, 2010.

[12] Y. X. Wang, S. B. Shan, C. Zhang, and P. P. Guo, "Seismic response of tunnel lining structure in a thick expansive soil stratum," *Tunnelling and Underground Space Technology*, vol. 88, pp. 250–259, 2019.

[13] L. Selen and K. K. Panthi, "A review of the testing approaches in swelling rock conditions at three different institutions," *IOP Conference Series: Earth and Environmental Science*, vol. 833, no. 1, article 012034, 2021.

[14] L. Selen, K. K. Panthi, M. B. Mørk, and B. E. Sørensen, "Compositional features and swelling potential of two weak rock types affecting their slake durability," *Geotechnics*, vol. 1, no. 1, pp. 172–191, 2021.

[15] D. Min and T. Mingshu, "Mechanism of dedolomitization and expansion of dolomitic rocks," *Cement and Concrete Research*, vol. 23, no. 6, pp. 1397–1408, 1993.

[16] C. Xu, Y. Zhang, and J. Yan, "Test study on the expansional properties of regenerated anhydrite rock," *IOP Conference Series: Earth and Environmental Science*, vol. 330, no. 4, article 042004, 2019.

[17] L. Li, L. He, and Y. Wang, "Test study on the expansion mechanical properties of regenerated anhydrite rock," *IOP Conference Series: Earth and Environmental Science*, vol. 358, no. 5, article 052029, 2019.

[18] Y. L. Wu, *Study on engineering geological characteristics of gypsum rock and its hazard mechanism to tunnel concrete structure*, China University of Geosciences, 2013.

[19] M. E. Bilir, "Swelling problems and triaxial swelling behavior of claystone: a case study in Tire, Turkey," *Scientific Research and Essays*, vol. 6, no. 5, pp. 1106–1116, 2011.

[20] Y. F. Arifin, M. Arsyad, and H. Muslim, "Swelling characteristics of compacted claystone-bentonite mixtures," *IOP Conference Series: Earth and Environmental Science*, vol. 933, no. 1, p. 012002, 2021.

[21] Y. Liu and S. K. Vanapalli, "Prediction of lateral swelling pressure behind retaining structure with expansive soil as backfill," *Soils and Foundations*, vol. 59, no. 1, pp. 176–195, 2019.

[22] U. Calik and E. Sadoglu, "Classification, shear strength, and durability of expansive clayey soil stabilized with lime and perlite," *Natural Hazards*, vol. 71, no. 3, pp. 1289–1303, 2014.

[23] S. Šliaupa, S. Lozovskis, J. Lazauskienė, and R. Šliaupienė, "Petrophysical and mechanical properties of the lower Silurian perspective oil/gas shales of Lithuania," *Journal of Natural Gas Science and Engineering*, vol. 79, p. 103336, 2020.

[24] L. L. Wang, R. W. Yang, S. Chanchole, and G. Q. Zhang, "The time-dependent swelling of argillaceous rock under resaturated conditions," *Applied Clay Science*, vol. 146, pp. 186–194, 2017.

[25] B. Zamin, H. Nasir, K. Mehmood, Q. Iqbal, A. Farooq, and M. Tufail, "An experimental study on the geotechnical, mineralogical, and swelling behavior of KPK expansive soils," *Advances in Civil Engineering*, vol. 2021, Article ID 8493091, 13 pages, 2021.

[26] M. Türköz, "Computer-controlled equipment for the direct measurement of the swell potential of expansive soils," *Arabian Journal of Geosciences*, vol. 12, no. 23, p. 743, 2019.

[27] R. Doostmohammadi, M. Moosavi, and B. N. Araabi, "A model for determining the cyclic swell-shrink behavior of argillaceous rock," *Applied Clay Science*, vol. 42, pp. 81–89, 2008.

[28] S. Azam, S. N. Abduljauwad, N. A. Al-Shayea, and O. S. B. Al-Amoudi, "Expansive characteristics of Gypsiferous/Anhydritic soil formations," *Engineering Geology*, vol. 51, no. 2, pp. 89–107, 1998.

[29] H. Ma, S. Chen, Y. Song, D. Yin, X. Li, and X. Li, "Experimental investigation into the effects of composition and microstructure on the tensile properties and failure characteristics of different gypsum rocks," *Scientific Reports*, vol. 11, no. 1, p. 14517, 2021.

[30] E.-S. S. Abu Seif, "Geotechnical characteristics of anhydrite/gypsum transformation in the middle Miocene Evaporites, Red Sea Coast, Egypt," *Arabian Journal for Science and Engineering*, vol. 39, no. 1, pp. 247–260, 2014.

[31] G. Testa and S. Lugli, "Gypsum-anhydrite transformations in Messinian evaporites of central Tuscany (Italy)," *Sedimentary Geology*, vol. 130, pp. 249–268, 2000.

[32] C. Kosztolanyi, J. Mullis, and M. Weidmann, "Measurements of the phase transformation temperature of gypsum-anhydrite, included in quartz, by microthermometry and Raman microprobe techniques," *Chemical Geology*, vol. 61, no. 1-4, pp. 19–28, 1987.

[33] F. Gutiérrez and A. H. Cooper, "Evaporite dissolution subsidence in the historical city of Calatayud, Spain: damage appraisal and prevention," *Natural Hazards*, vol. 25, no. 3, pp. 259–288, 2002.

[34] N. Darıcı and S. Özel, "Examination of the structural characteristics arising in gypsums by the GPR and MASW methods (Sivas, Turkey)," *Natural Hazards*, vol. 93, no. 2, pp. 661–676, 2018.

[35] F. Rauh, G. Spaun, and K. Thuro, "Assessment of the swelling potential of anhydrite in tunnelling projects," in *The Geological Society of London. IAEG Engineering geology for tomorrows cities*, vol. 9, Proceedings of the 10th IAEG International Congress, Nottingham, United Kingdom, 2006.

[36] E. E. Alonso, I. R. Berdugo, and A. Ramon, "Extreme expansive phenomena in Anhydritic-Gypsiferous claystone: the case of Lilla tunnel," *Géotechnique*, vol. 63, no. 7, pp. 584–612, 2013.

[37] Z. Chang, F. Catani, F. Huang et al., "Landslide susceptibility prediction using slope unit-based machine learning models considering the heterogeneity of conditioning factors," *Journal of Rock Mechanics and Geotechnical Engineering*, 2022.

[38] F. Huang, J. Zhang, C. Zhou, Y. Wang, J. Huang, and L. Zhu, "A deep learning algorithm using a fully connected sparse autoencoder neural network for landslide susceptibility prediction," *Landslides*, vol. 17, no. 1, pp. 217–229, 2020.

[39] The First Railway survey and Design Institute, *Tb10038-2001 Code for special geotechnical investigation of railway engineering*, China Railway Publishing House, Beijing, 2001.

[40] F. Beaugnon, S. Quiligotti, S. Chevreux, and G. Wallez, "On the monoclinic distortion of _β_ -anhydrite $CaSO_4$," *Solid State Sciences*, vol. 108, p. 106399, 2020.

[41] A. Liu, S. Liu, P. Liu, and K. Wang, "Water sorption on coal: effects of oxygen-containing function groups and pore structure," *International Journal of Coal Science & Technology*, vol. 8, no. 5, pp. 983–1002, 2021.

[42] S. Cao, W. Yin, B. Yang et al., "Insights into the influence of temperature on the adsorption behavior of sodium oleate

and its response to flotation of quartz," *International Journal of Mining Science and Technology*, vol. 32, no. 2, pp. 399–409, 2022.

[43] G. Han, S. Wen, H. Wang, and Q. Feng, "Sulfidization regulation of cuprite by pre-oxidation using sodium hypochlorite as an oxidant," *International Journal of Mining Science and Technology*, vol. 31, no. 6, pp. 1117–1128, 2021.

[44] G. Simsek Franci, "Handheld X-ray fluorescence (XRF) versus wavelength dispersive XRF: characterization of Chinese blue-and-white porcelain sherds using handheld and laboratory-type XRF instruments," *Applied Spectroscopy*, vol. 74, no. 3, pp. 314–322, 2020.

[45] F. Li, L. Ge, Z. Tang, Y. Chen, and J. Wang, "Recent developments on XRF spectra evaluation," *Applied Spectroscopy Reviews*, vol. 55, no. 4, pp. 263–287, 2020.

[46] G. Kontsevich and L. Löwemark, "Corascope: software assisted XRF scan merging," *Computers & Geosciences*, vol. 156, p. 104906, 2021.

[47] L. Van Loon, S. McIntyre, N. Sherry, M. Bauer, and N. Banerjee, "User-friendly software for the analysis of complex XRF spectra," *Microscopy and Microanalysis*, vol. 26, no. S2, pp. 510–513, 2020.

[48] J. Liu, Q. Zhang, F. Chen, and T. Li, "Study on expansion mechanism of mudstone under structural strength," *IOP Conference Series: Earth and Environmental Science*, vol. 267, no. 5, article 052005, 2019.

[49] A. V. Smagin, A. S. Bashina, V. V. Klyueva, and A. V. Kubareva, "Thermal desorption analysis of effective specific soil surface area," *Eurasian Soil Science*, vol. 50, no. 12, pp. 1428–1434, 2017.

[50] J. She, Z. Lu, H. Yao, R. Fang, and S. Xian, "Experimental study on the swelling behavior of expansive soil at different depths under unidirectional seepage," *Applied Sciences*, vol. 9, no. 6, p. 1233, 2019.

[51] Ministry of Water Resources, PRC, *Geotechnical test method standard: GB/T 50123-2019*, China Planning Press, Beijing, 2019.

[52] Y. I. Mawlood and R. A. Hummadi, "Large-scale model swelling potential of expansive soils in comparison with oedometer swelling methods," *Iranian Journal of Science and Technology, Transactions of Civil Engineering*, vol. 44, no. 4, pp. 1283–1293, 2020.

[53] S. Selvakumar and B. Soundara, "Swelling behaviour of expansive soils with recycled geofoam granules column inclusion," *Geotextiles and Geomembranes*, vol. 47, no. 1, pp. 1–11, 2019.

[54] B. Lin and A. B. Cerato, "Prediction of expansive soil swelling based on four micro-scale properties," *Bulletin of Engineering Geology and the Environment*, vol. 71, no. 1, pp. 71–78, 2012.

[55] Z. Liu, M. Li, F. Yan, and H. Luo, "Study on influence factors of water content of expansive soil in canal slope based on Grey correlation model," *IOP Conference Series: Earth and Environmental Science*, vol. 304, no. 2, article 022027, 2019.

[56] T. Ma, C. Yao, Y. Dong, P. Yi, and C. Wei, "Physicochemical approach to evaluating the swelling pressure of expansive soils," *Applied Clay Science*, vol. 172, pp. 85–95, 2019.

[57] H. Elsaidy, W. M. Yan, and M. J. Pender, "A novel formula for the prediction of swelling pressure of compacted expansive soils," *Géotechnique Letters*, vol. 9, no. 3, pp. 231–237, 2019.

[58] S. Wei, C. Wang, Y. Yang, and M. Wang, "Physical and mechanical properties of gypsum-like rock materials," *Advances in Civil Engineering*, vol. 2020, Article ID 3703706, 17 pages, 2020.

[59] Z. Li, K. Xu, J. Peng, J. Wang, X. Ma, and J. Niu, "Investigation on the deterioration mechanism of recycled plaster," *Advances in Materials Science and Engineering*, vol. 2018, Article ID 4791451, 8 pages, 2018.

[60] S. Kwon, H. Hwang, and Y. Lee, "Effect of pressure treatment on the specific surface area in kaolin group minerals," *Crystals*, vol. 9, no. 10, p. 528, 2019.

[61] V. Danielik, P. Fellner, M. Králik et al., "Relation between the reactivity and surface area of gypsum," *Journal of Molecular Liquids*, vol. 283, pp. 763–771, 2019.

[62] M. Mastalerz, L. Wei, A. Drobniak, A. Schimmelmann, and J. Schieber, "Responses of specific surface area and micro- and mesopore characteristics of shale and coal to heating at elevated hydrostatic and lithostatic pressures," *International Journal of Coal Geology*, vol. 197, pp. 20–30, 2018.

[63] H. Tang, J. Wang, L. Zhang et al., "Testing method and controlling factors of specific surface area of shales," *Journal of Petroleum Science and Engineering*, vol. 143, pp. 1–7, 2016.

[64] R. A. Kleiv and M. Thornhill, "The effect of mechanical activation in the production of olivine surface area," *Minerals Engineering*, vol. 89, pp. 19–23, 2016.

[65] E.-J. Yang, Z.-T. Zeng, H.-Y. Mo, T. Hu, C.-L. Yang, and S.-H. Tang, "Analysis of bound water and its influence factors in mixed clayey soils," *Water*, vol. 13, no. 21, p. 2991, 2021.

[66] S. A. Schweizer, C. W. Mueller, C. Höschen, P. Ivanov, and I. Kögel-Knabner, "The role of clay content and mineral surface area for soil organic carbon storage in an arable toposequence," *Biogeochemistry*, vol. 156, no. 3, pp. 401–420, 2021.

[67] Q. Huang, J. Li, S. Liu, and G. Wang, "Experimental study on the adverse effect of gel fracturing fluid on gas sorption behavior for Illinois coal," *International Journal of Coal Science & Technology*, vol. 8, no. 6, pp. 1250–1261, 2021.

[68] Q. Wang, J. Liu, P. Wang, M. Yu, L. Wang, and J. Yao, "Influence of specific surface area on sulfate attack–induced expansion of cement-treated aggregates," *Bulletin of Engineering Geology and the Environment*, vol. 80, no. 6, pp. 4841–4854, 2021.

[69] Z. Li, K. Xu, J. Peng, J. Wang, J. Zhang, and Q. Li, "Influence of the heating temperature and fineness on the hydration and mechanical property of recycled gypsum plaster," *Advances in Materials Science and Engineering*, vol. 2021, Article ID 7520378, 12 pages, 2021.

[70] J. F. Gomes, M. Davies, P. Smith, and F. Jones, "The formation of desilication products in the presence of kaolinite and halloysite - the role of surface area," *Hydrometallurgy*, vol. 203, p. 105643, 2021.